Proceedings of 20th International Congress on Acoustics, ICA 2010

23-27 August 2010, Sydney, Australia

Investigation on the cause of instability in time domain acoustic BEM using the wave vector concept

Hae-Won Jang and Jeong-Guon Ih

Centre for Noise and Vibration Control, Korea Advanced Institute of Science and Technology, Daejeon 305-701, Korea

PACS: 43.20.Px Transient radiation and scattering

ABSTRACT

Time domain boundary element method (TBEM) employs the time marching field integral algorithm to solve transient problems. Because it usually suffers from the instability, various methods to treat such an instability problem have been attempted, but the onset time of instability is only delayed and the instability still occurs under some conditions. This paper describes our recent effort to stabilize the TBEM calculation by the wave vector filtering. Time responses are composed of the sum of wave vectors which are amplified with the magnitudes of their eigenvalues at each time step. As a simulation example, the sound propagation from a point source in a rigid box was taken. Instability occurred by the numerical error in the resonant modes. Stabilization of TBEM calculation could be achieved by excluding wave vectors, of which eigenvalues were larger than one.

INTRODUCTION

Time domain boundary element method (TBEM), which is based on the retarded potential equation, employs the time marching algorithm. This method has a good potential to be applied to various transient wave propagation problems in acoustics, electromagnetics, geophysics, elastodynamics, etc. General derivation of boundary integral formulation for the transient 3-D wave propagation problem can be found in [1,2]. Examples of sound propagation problems can be seen in [3,4]. The major obstacle prohibiting the use of the TBEM widely is due to the instability.

The instability seems to be related with the internal resonance frequencies of an enclosed body in the scattering problem [5]. Numerical approximation error may enlarge the decay rate of internal resonant modes to be larger than one, leading to the instability [6]. The condition of instability might be mathematically explained by the eigenvalues of a single iterative matrix of the implicit formulation [7].

Various methods have been suggested to stabilize the TBEM calculations. Methods using the averaging scheme, which filters the temporal and spatial high frequency components by the solution smoothing, were reported to improve the stability [8,9]. The central difference scheme used for the time derivative was found to decrease the instability by suppressing the high frequency unstable components [10]. The temporal and spatial interpolation functions [11,12] and the Galerkin method [13] were introduced to suppress the instability, which described the causality of the wave propagation phenomenon. A combined integral equation incorporating the time domain Burton-Miller formulation was introduced to avoid the instability at the internal resonances in the exterior problems [14,15]. Although the foregoing methods tried to stabilize the computation by suppressing some causes of instability, the stability on the entire time-domain could not be assured in general. The onset time of instability is only delayed under some special conditions, but the instability itself usually occurs for some time later yet.

In this paper, we tried to physically describe the cause of instability and suggest a stabilization method employing the wave vector filtering. The present stabilization method is different from other previous methods in the adjustment of unstable wave vectors during the calculation. Wave vectors, which constitute the natural behaviour of the system response in time domain, were calculated from eigenvectors of a single iterative matrix of TBEM equation. In every time step, the time response was projected into the wave vector space by the least square method and the unstable wave vectors were truncated. As a simulation example, the sound propagation from a point source in a rigid box was considered.

FORMULATION

The following Kirchhoff integral equation provides the basis of the acoustic TBEM [1]:

$$c(\boldsymbol{r}_0)p(\boldsymbol{r}_0,t)=\frac{1}{4\pi}\int_S\left[\frac{1}{R^2}\frac{\partial R}{\partial n}\{p(\boldsymbol{r}_s,t_{ret})+\frac{R}{c_0}\frac{\partial p}{\partial t}(\boldsymbol{r}_s,t_{ret})\}-\frac{1}{R}\frac{\partial p}{\partial n}(\boldsymbol{r}_s,t_{ret})\right]dS\,. \quad (1)$$

Here, $c(\boldsymbol{r}_0)$ denotes the solid angle, $p(\boldsymbol{r}, t)$ is the pressure at location $\boldsymbol{r}$ and at time t, $R=|\boldsymbol{r}_0-\boldsymbol{r}_s|$ the distance between field point $\boldsymbol{r}_0$ and surface point $\boldsymbol{r}_s$, $t_{ret}=t-R/c$ the retarded time, and $(\partial/\partial n)$ the outer normal derivative on the surface.

For the surface points, the discretized Kirchhoff integral becomes

$$\boldsymbol{C}\boldsymbol{P}_n=\sum_{i=0}^{W}\left[\boldsymbol{\alpha}_i\boldsymbol{P}_{n-i}+\boldsymbol{\beta}_i\left(\frac{\partial\boldsymbol{P}}{\partial t}\right)_{n-i}\right]+\sum_{i=0}^{W}\left[\gamma_i\left(\frac{\partial\boldsymbol{P}}{\partial n}\right)_{n-i}\right], \quad (2)$$

where $\boldsymbol{C}$ is the diagonal matrix containing the solid angles, $\boldsymbol{P}_n$ the surface pressure vector at $n\Delta t$, $\boldsymbol{\alpha}_i$, $\boldsymbol{\beta}_i$, γ_i are the coefficient matrices of the dipole and monopole terms for the surface

variables at $(n\text{-}i)\Delta t$, W the maximum retarded time step which is calculated from the geometric size of the system.

If the mixed boundary condition is assigned, TBEM formulation can be expressed as

$$\{\boldsymbol{Y}\}_n = \sum_{i=1}^{m+W} \boldsymbol{A}_i \{\boldsymbol{Y}\}_{n-i} + \sum_{i=0}^{W+1} \boldsymbol{B}_i \{\boldsymbol{X}\}_{n-i} \,, \tag{3}$$

where $\boldsymbol{A}_i$, $\boldsymbol{B}_i$ are the rearranged coefficient matrices. The time derivative is discretized by the 1st order central difference scheme. In Eq. (3), a finite impulse response (FIR) filter is used to obtain an impulse response for the impedance boundary condition, for which m denotes its length. The input vector $\{\boldsymbol{X}\}$ and the output vector $\{\boldsymbol{Y}\}$ are respectively given by

$$\{\boldsymbol{X}\}_{n-i} = \left[\left(\boldsymbol{P}|_D\right) \ \left(\frac{\partial \boldsymbol{P}}{\partial n}\bigg|_N\right) \right]^T_{n-i}, \{\boldsymbol{Y}\}_{n-i} = \left[\left(\frac{\partial \boldsymbol{P}}{\partial n}\bigg|_D\right) \ \left(\boldsymbol{P}|_N\right) \ \left(\boldsymbol{P}|_A\right) \right]^T_{n-i} . \tag{4a,b}$$

Here, the notations $(..)|_D$, $(..)|_N$, $(..)|_A$ denote the surface variable vectors for the Dirichlet, Neumann, and impedance boundary condition, respectively.

Equation (3) can be expressed as the recursive structure with single feedback as shown in Fig. 1. If the impedance boundary condition is modeled by an infinite impulse response (IIR) filter, the calculation can be modeled with a double feedback structure. It can be noted that the calculation algorithm resembles the multi-input multi-output (MIMO) IIR filter.

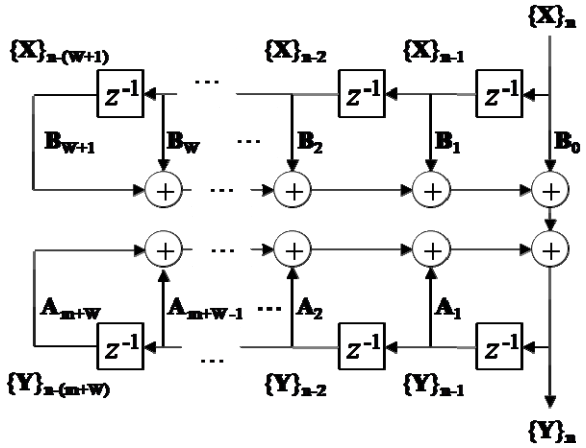

Figure 1. A block diagram of the recursive TBEM algorithm with a single feedback.

ANALYSIS OF TIME-DOMAIN BE MODEL

System equation

Equation (3) can be easily reformed into the following canonical form [7]:

$$\begin{bmatrix} \{\boldsymbol{Y}\}_n \\ \{\boldsymbol{Y}\}_{n-1} \\ \vdots \\ \vdots \\ \{\boldsymbol{Y}\}_{n-(W+m-1)} \end{bmatrix} = \begin{bmatrix} \boldsymbol{A}_1 & \boldsymbol{A}_2 & \cdots & & \boldsymbol{A}_{W+m} \\ \boldsymbol{I} & \boldsymbol{0} & & \cdots & \boldsymbol{0} \\ \boldsymbol{0} & \boldsymbol{I} & \boldsymbol{0} & \cdots & \vdots \\ \vdots & \boldsymbol{0} & \cdots & \boldsymbol{0} & \vdots \\ \boldsymbol{0} & \cdots & \boldsymbol{0} & \boldsymbol{I} & \boldsymbol{0} \end{bmatrix} \begin{bmatrix} \{\boldsymbol{Y}\}_{n-1} \\ \{\boldsymbol{Y}\}_{n-2} \\ \vdots \\ \vdots \\ \{\boldsymbol{Y}\}_{n-(W+m)} \end{bmatrix} + \begin{bmatrix} \boldsymbol{I} \\ 0 \\ \vdots \\ \vdots \\ 0 \end{bmatrix} \cdot \sum_{i=0}^{W+1} \boldsymbol{B}_i \{\boldsymbol{X}\}_{n-i} \,, \tag{5a}$$

or

$$\langle \boldsymbol{Y} \rangle_n = \boldsymbol{M} \langle \boldsymbol{Y} \rangle_{n-1} + \langle \boldsymbol{X} \rangle_n \,. \tag{5b}$$

The response $\langle \boldsymbol{Y} \rangle_n$ represents the sequential distribution of surface variables within the time of $(m+W)\Delta t$. The input $\langle \boldsymbol{X} \rangle_n$ is given by the boundary conditions. To investigate the response behavior of time-domain BE model (TBE model), the response is assumed to be exponential function as

$$\langle \boldsymbol{Y} \rangle_n = \exp\left((-\alpha - j\omega) \cdot n\Delta t\right) \cdot \boldsymbol{u} \,, \tag{6}$$

where α is a constant related to the attenuation and $\boldsymbol{u}$ is a constant vector. Substituting Eq. (6) into Eq. (5b) and assuming that $\langle \boldsymbol{X} \rangle_n$ is given as zero, the following eigen-equation can be formulated:

$$(\boldsymbol{M} - \lambda \boldsymbol{I})\boldsymbol{u} = 0 \,, \qquad \lambda = \exp\left((-\alpha - j\omega)\Delta t\right) . \tag{7a,b}$$

This approach is applicable only to the recursive structure with a single feedback.

The solutions of Eq. (7a) determine the characteristics of natural behavior of the response. Solutions are the complex conjugate pairs because $\boldsymbol{M}$ is not symmetric. Physically, these conjugate pairs represent the incoming and outgoing waves. Due to complex expression, eigen-solutions cannot be applied directly to analyze the TBE model. Accordingly, the eigen-equation should be separated into real and imaginary parts as

$$\boldsymbol{M}^l \boldsymbol{u}_i = \left(\lambda_i\right)^l \cdot \boldsymbol{u}_i \,, \tag{8a}$$

$$\boldsymbol{M}^l \ \mathrm{Re}\left(\boldsymbol{u}_i\right) = \mathrm{Re}\left(\lambda_i^l\right) \cdot \mathrm{Re}\left(\boldsymbol{u}_i\right) - \mathrm{Im}\left(\lambda_i^l\right) \cdot \mathrm{Im}\left(\boldsymbol{u}_i\right) \,, \tag{8b}$$

$$\boldsymbol{M}^l \ \mathrm{Im}\left(\boldsymbol{u}_i\right) = \mathrm{Re}\left(\lambda_i^l\right) \cdot \mathrm{Im}\left(\boldsymbol{u}_i\right) + \mathrm{Im}\left(\lambda_i^l\right) \cdot \mathrm{Re}\left(\boldsymbol{u}_i\right) \,, \tag{8c}$$

where $\boldsymbol{u}_i$, λ_i are the i^{th} eigenvector and eigenvalue, respectively, and l denotes the elapsed time step.

Physical description of the solutions

The eigen-vectors determine the time-varying natural modes of the response $\langle \boldsymbol{Y} \rangle_n$. In other words, the response vectors are expressed in time domain by the complicated interaction between real and imaginary parts of eigenvectors which are expected to vary in time with a spatial distribution of surface variables within the maximum time delay. In this sense, real and imaginary parts of eigenvectors can be called the time-domain wave vectors.

The magnitude of eigenvalue $|\lambda|$ includes the decay rate of the corresponding wave vector at a time step. The time response can diverge exponentially due to the decay rate larger than one. The condition of divergence can be defined as

$$\boldsymbol{q}_i^T \cdot \langle \boldsymbol{Y} \rangle_k \neq 0 \quad \text{for} \ \ |\lambda_i| > 1 \,, \tag{9}$$

where $\boldsymbol{q}_i$ denotes the time-domain wave vectors.

The interactive process in Eqs. (8b) and (8c) should be repeated every time satisfying the condition of $\arg(\lambda_i^l) = -l\omega\Delta t = 2n\pi$. The frequency of wave vector can be calculated from the phase of corresponding eigenvalue as [6]

$$f_i = \frac{1}{l\Delta t} = \frac{\arg\left(\lambda_i\right)}{2\pi \cdot \Delta t} \,. \tag{10}$$

Instability condition

In the former section, it was mentioned that the instability in the TBEM calculation was caused from the overestimated decay rate of some eigen-modes to be larger than one. This means that the numerical errors in dealing with the resonant

modes with very small damping would be main cause of the instability. Even in the exterior problems having the geometric divergence, the unphysical damping property of internal resonances can cause the instability [6]. Such an overestimation error may be larger for the problem with the mixed boundary conditions because the coefficient matrices are more complicated than the problems with simple boundary condition involved with radiation and scattering problems. Most of previous studies focused on the reduction of overestimated unphysical decay rate, but their algorithm worked only under specific condition. The consequence was only a delay of the onset time of instability, so the instability would eventually occur. During the TBEM calculation, the instability occurs due to aforementioned reason and also the unstable complementary wave vector develops because of the errors in estimating the high order wave vector modes constructing a rank-deficient wave vector space. The present study focused on the elimination of unstable wave vectors.

FILTERING FOR STABILIZATION

Wave vector expansion

For the stabilization, one should first calculate the wave vectors of the response $\langle \boldsymbol{Y} \rangle_n$ at every time step. In this study, the response is projected to the wave vector space in the least square sense as

$$\{\boldsymbol{c}\}_k = \boldsymbol{U}_1 \boldsymbol{\Sigma}^+ \boldsymbol{U}_2^* \langle \boldsymbol{Y} \rangle_k = \boldsymbol{Q}^+ \langle \boldsymbol{Y} \rangle_k \,. \tag{11}$$

Here, $\boldsymbol{Q} = [\boldsymbol{q}_1\ \boldsymbol{q}_2 \ldots \boldsymbol{q}_n]$ denotes the wave vector space, $\boldsymbol{q}_i$ is the wave vector, $\{\boldsymbol{c}\}_k$ the coefficients vector of each wave vector, $\boldsymbol{U}_1$, $\boldsymbol{U}_2$ the unitary matrices called right and left singular vectors, respectively, $\boldsymbol{\Sigma}$ the diagonal matrix containing the non-negative real singular value. However, the wave vector space is generally rank-deficient, which results the response being given as

$$\langle \boldsymbol{Y} \rangle_k = \boldsymbol{Q}\{\boldsymbol{c}\}_k + \left(\boldsymbol{I} - \boldsymbol{Q}\boldsymbol{Q}^+\right)\langle \boldsymbol{Y} \rangle_k \,, \tag{12}$$

where $(\boldsymbol{I}\text{-}\boldsymbol{Q}\boldsymbol{Q}^+)\langle \boldsymbol{Y} \rangle_k$ means the complementary wave vector space to $\boldsymbol{Q}$. With the aid of the least square method, the response can be decomposed into two components of wave vector space and its complementary space minimizing the residue of wave vector expansion to be $(\boldsymbol{I}\text{-}\boldsymbol{Q}\boldsymbol{Q}^+)\langle \boldsymbol{Y} \rangle_k$.

Elimination of unstable wave vectors

It is thought that the response by the TBEM calculation can be stabilized by discarding the unstable wave vectors. At every time step, unstable wave vectors can be nullified by the truncation as

$$\langle \boldsymbol{Y} \rangle_k^* = \boldsymbol{Q} \cdot \boldsymbol{F} \cdot \{\boldsymbol{c}\}_k + \left(\boldsymbol{I} - \boldsymbol{Q}\boldsymbol{Q}^+\right)\langle \boldsymbol{Y} \rangle_k \,, \tag{13a}$$

$$\boldsymbol{F} = diag\left(1,\ \cdots\ 1,\ 0,\ \cdots\ 0\right), \tag{13b}$$

$$\{\boldsymbol{Y}\}_{k+1} = \left[\boldsymbol{A}_1\ \ \boldsymbol{A}_2\ \ \ldots\ \ \boldsymbol{A}_{W+m}\right]\langle \boldsymbol{Y} \rangle_k^* + \sum_{i=0}^{W+1} \boldsymbol{B}_i \{\boldsymbol{X}\}_{n-i} \,, \tag{13c}$$

$$\langle \boldsymbol{Y} \rangle_{k+1} = \left[\{\boldsymbol{Y}\}_{k+1}^T\ \ \{\boldsymbol{Y}\}_k^T\ \ \ldots\ \ \{\boldsymbol{Y}\}_{k-(W+m-2)}^T\right]^T, \tag{13d}$$

where $\langle \boldsymbol{Y} \rangle_k^*$ denotes the truncated response. Although the deviation of truncated response from the initial one is small if the frequencies of unstable wave vectors are much higher than the frequencies related to the mesh size and time step, the fidelity of the stabilized response would be in general degraded by losing the unstable wave vector components.

DEMONSTRATION EXAMPLE

As a demonstration example, the sound propagation by a point source within a rigid parallelepiped box was taken. Figure 2 illustrates the geometric size of the box, which is 0.9m x 1.1m x 0.7m, and the BE model composed of 96 nodes and 188 linear triangular element. The maximum element size was 0.32 m, which suggests the reliable frequency range below 270 Hz by λ/4 criterion.

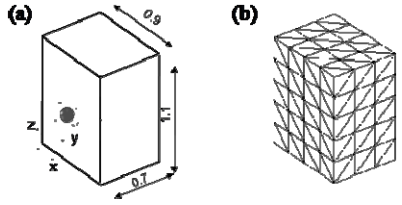

Figure 2. (a) A rigid parallelepiped box with a point source at (0.1, 0.2, 0.3) m, (b) BE model (96 nodes, 188 linear triangular elements).

Time step size Δt was selected as 0.2 ms ($c\Delta t/\Delta h$ = 0.35) satisfying the CFL condition. Maximum time delay was set as $24{\cdot}\Delta t$, so the number of wave vector modes in the TBE model was 2304 ($24{\cdot}\Delta t$ x 96 nodes).

Octave band impulse was given at a point source located at (0.1, 0.2, 0.3) in m as follows:

$$p_i(\boldsymbol{r}_s, t) = \int_{-\infty}^{\infty} \left\{ h(f) \cdot \frac{\exp(-jkR)}{R} \right\} \cdot \exp\left(j \cdot 2\pi f \cdot t\right) df \,. \tag{14}$$

Here, $h(f)$ denotes the octave band pass filter centered at 63 Hz and k is the wave number, R the distance between the point source and a surface point.

In the test example, there were only 5 unstable wave vectors, of which eigenvalues were exceeding one. Table 1 summarized the characteristics of those unstable wave vectors.

Table 1. Characteristics of unstable wave vectors.

order	$\lvert\lambda\rvert$	f_i=arg(λ)/2πΔt, Hz	Wave vector shape
5	1.0001	0	(0, 0, 0)
111,112	1.0199	1328	(1, 1, 2)
129,130	1.0167	1308	(2, 1, 2)

Frequencies of all these wave vectors except the 5th one were much higher than the error limit frequency given from λ/4 criterion. One can find that the frequency of observed wave vector shape is much lower than the frequency of the corresponding eigenvalue. This reveals that the observed unstable wave vectors are spatially aliased due to the finiteness of boundary elements. For instance, the (1, 1, 2) wave vector appears actually at 446 Hz which is different from the eigenfrequency. Figure 3 depicts the 111th wave vector, as an example of unstable wave vectors, and one can see that its response increase gradually as the time elapses.

Calculated impulse responses in 63 Hz octave band are presented in Fig. 4. An exponential divergence phenomenon can be observed. To monitor the correlation between the response $\langle \boldsymbol{Y} \rangle_k$ and unstable wave vectors $\boldsymbol{q}_i$, the modal assurance criterion (MAC), which has been widely used to indicate the consistency of mode shapes in modal analysis [16], was calculated at each time step. The MAC value is defined as

$$MAC\left(\langle \boldsymbol{Y} \rangle_k, \boldsymbol{q}_i\right) = \frac{\left|\langle \boldsymbol{Y} \rangle_k^T \boldsymbol{q}_i\right|^2}{\left|\langle \boldsymbol{Y} \rangle_k^T \langle \boldsymbol{Y} \rangle_k\right| \left|\boldsymbol{q}_i^T \cdot \boldsymbol{q}_i\right|} . \quad (15)$$

Time history of MAC value for the unstable response is shown in Fig. 5, which indicates the time span of the dominance of the unstable wave vector. In this example, the most dominant unstable wave vectors are the 111, 112th vectors because their decay rates are largest one of all. One can observe that the 5th wave vector does not contribute to the onset of the instability.

Figure 6 displays a successfully stabilized response as a result of the wave vector filtering, which shows almost perfect match with the inverse Fourier transform of frequency-domain BEM (FBEM). Such a good agreement is due to the fact that frequencies of unstable wave vectors are much higher than the excited frequency. The resultant correlation with unstable wave vectors can be seen in Fig. 7, which depicts the elimination of problematic vectors during the calculation step.

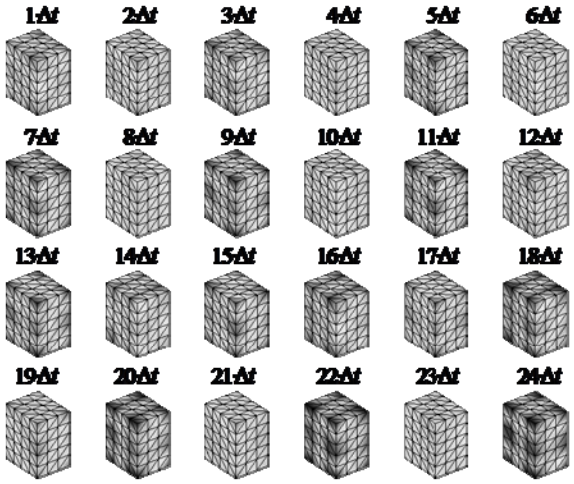

Figure 3. Shape of the 111th wave vector.

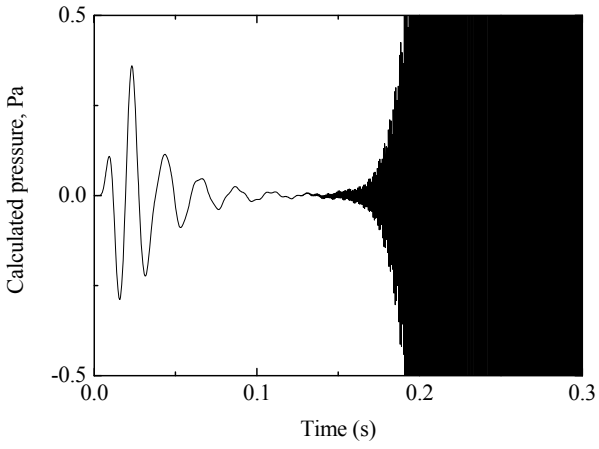

Figure 4. Calculated surface pressure at (0.467, 0.450, 1.10) m subject to an impulse excitation at 63 Hz octave band.

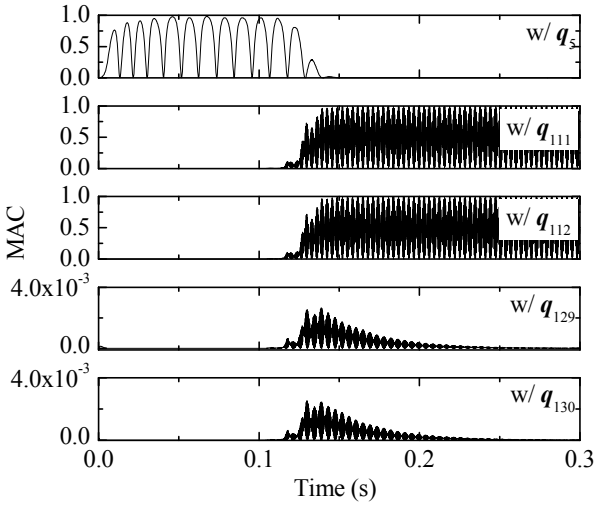

Figure 5. Time history of MAC values of unstable wave vectors and calculated response ‹***Y***›.

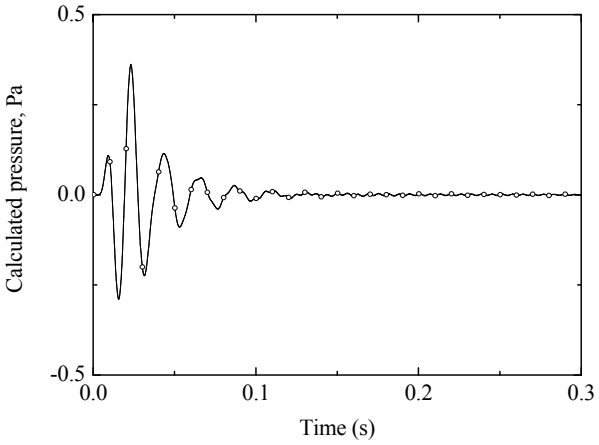

Figure 6. Stabilized surface pressure at (0.467, 0.450, 1.10) m for an impulse excitation at 63 Hz octave band. —, TBEM; —○—, FBEM.

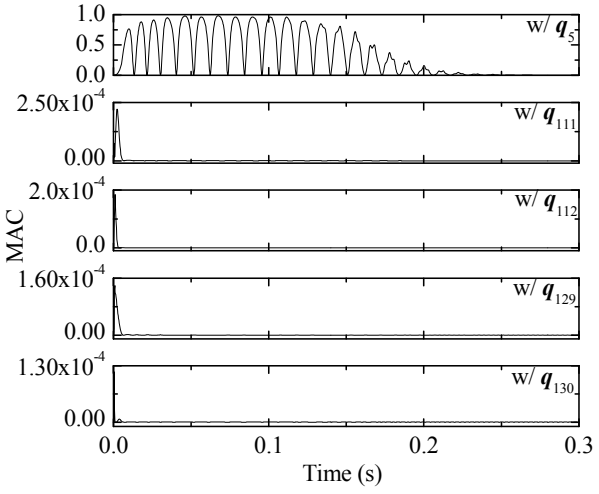

Figure 7. Time history of MAC values of unstable wave vectors and stabilized response ‹***Y***›.

CONCLUSIONING REMARKS

Numerical characteristics of TBEM algorithm were explained physically and the stabilization method by the wave vector filtering was suggested. It was discussed that wave vectors, which are real and imaginary parts of eigenvectors of time-marching iterative matrix, represent natural behavior of the system response at each time step. Each of them was multiplied with the corresponding complex eigenvalue. It was concluded that the instability in TBEM was caused from some wave vector modes having larger decay rates than one.

Wave vector filtering was used for the computational stabilization. To this end, the least square method was adopted in expanding the response to the wave vector space and MAC value was employed to find the correlation between the response and the unstable wave vectors. Unstable wave vectors were excluded counting the truncation errors. In the simulation example, the proposed stabilization method was successful in dealing with the problem having Neumann boundary condition. It is thought that the present idea can be extendedly applied to more general problems having the mixed boundary condition.

ACKNOWLEDGMENT

This work was partially supported by BK21 project.

REFERENCES

1. P.H.L. Groenenboom, “Wave propagation phenomena,” *Progress in Boundary Element Methods* (Pentech, London, 1983) pp. 24-52
2. W.J. Mansur and C.A. Brebbia, “Formulation of boundary element method for transient problems governed by the scalar wave equation,” *Appl. Math. Modelling* **6**, 307-311 (1982)
3. K.M. Mitzner, “Numerical solution for transient scattering from a hard surface-retarded potential techniques,” *J. Acoust. Soc. Am.* **42**, 391–397 (1967)
4. R.P. Shaw, “Transient acoustic scattering by a free (pressure release) sphere,” *J. Sound Vib.* **20**, 321-331 (1972)
5. P.D. Smith, “Instabilities in time marching methods for scattering: cause and rectification,” *Electromagnetics* **10**, 439-451 (1990)
6. H. Wang, D.J. Henwood, P.J. Harris, and R. Chakrabarti, “Concerning the cause of instability in time stepping boundary element methods applied to the exterior acoustic problem,” *J. Sound Vib.* **305**, 298-297 (2007)
7. S.J. Dodson, S.P. Walker, and M.J. Bluck, “Implicitness and stability of time domain integral equation scattering analyses,” *Appl. Comput. Electrom.* **13**, 291-301 (1997)
8. B.P. Rynne and P.D. Smith, “Stability of time marching algorithms for the electric field integral equation,” *J. Electromagnet. Wave.* **4**, 1181-1205 (1990).
9. P.J. Davies and B. Duncan, “Averaging techniques for time-marching schemes for retarded potential integral equations,” *Appl. Numer. Math.* **23**, 291-310 (1997)
10. B.P. Rynne, “Stability and convergence of time marching methods in scattering problems,” *IMA J. Appl. Math.* **35**, 297-310 (1985)
11. A. Peirce and E. Siebrits, “Stability analysis and design of time-stepping schemes for general elastodynamic boundary element models,” *Int. J. Numer. Meth. Engng.* **40**, 319-342 (1997)
12. G. Yu, W.J. Mansur, and J.A.M. Carrer, “A linear θ method applied to 2D time-domain BEM,” *Commun. Numer. Meth. Engng.* **14**, 1171-1179 (1998)
13. G. Yu, W.J. Mansur, J.A.M. Carrer, and L. Gong, “Stability of Galerkin and collocation time domain boundary element methods as applied to the scalar wave equation,” *Comput. Struct.* **74**, 495-506 (2000)
14. A.A. Ergin, B. Shanker, and E. Michielssen, “Analysis of transient wave scattering from rigid bodies using a Burton-Miller approach,” *J. Acoust. Soc. Am.* **106**, 2396-2404 (1999)
15. D.J. Chappell, P.J. Harris, D. Henwood, and R. Chakrabarti, “A stable boundary element method for modeling transient acoustic radiation,” *J. Acoust. Soc. Am.* **120**, 76-80 (2006)
16. R.J. Allemang, “The modal assurance criterion –Twenty years of use and abuse,” *Sound and Vib.* 14-21, August (2003)